



Feasibility of lattice radiotherapy using proton and carbon-ion pencil beam for sinonasal malignancy

Dong Yang^{1,2,3}, Weiwei Wang^{1,2,3}, Jiyi Hu^{2,3,4}, Weixu Hu^{2,3,4}, Xiyu Zhang^{1,2,3}, Xiaodong Wu^{1,2,3}, Jiade J. Lu^{2,3,4}, Lin Kong^{2,3,4}

¹Department of Medical Physics, Shanghai Proton and Heavy Ion Center, Fudan University Cancer Hospital, Shanghai, China; ²Shanghai Key Laboratory of Radiation Oncology (20dz2261000), Shanghai, China; ³Shanghai Engineering Research Center of Proton and Heavy Ion Radiation Therapy, Shanghai, China; ⁴Department of Radiation Oncology, Shanghai Proton and Heavy Ion Center, Fudan University Cancer Hospital, Shanghai, China

Contributions: (I) Conception and design: L Kong, JJ Lu; (II) Administrative support: L Kong, JJ Lu, X Wu; (III) Provision of study materials or patients: J Hu, W Hu; (IV) Collection and assembly of data: D Yang; (V) Data analysis and interpretation: D Yang, L Kong, W Wang, X Zhang; (VI) Manuscript writing: All authors; (VII) Final approval of manuscript: All authors.

Correspondence to: Jiade J. Lu; Lin Kong. Department of Radiation Oncology, Shanghai Proton and Heavy Ion Center, Fudan University Cancer Hospital, 4365 Kangxin Road, Pudong, Shanghai 201321, China. Email: jiade.lu@sphic.org.cn; lin.kong@sphic.org.cn.

Background: Sinonasal malignancies are a treatment challenge because of their complex anatomy and close proximity to organs at risk (OARs). We aimed to investigate the feasibility of lattice radiotherapy (LRT) using pencil beam scanning (PBS) proton or carbon-ion beams in the treatment of sinonasal malignancies.

Methods: A total of 10 patients with nonoperative and bulky sinonasal adenoid cystic carcinomas (ACC) were enrolled. Spherical vertices with a 1 cm diameter and average center-to-center (c-t-c) distance of 3.51 cm were delineated within the gross tumor volumes (GTVs). The prescription doses were 15 Gy[relative biologic effectiveness (RBE)] to the vertices and 3 to 3.5 Gy(RBE) to the periphery, delivered as clinical target volume boosts (CTVboosts) in 1 fraction. Photon, proton, and carbon-ion LRT plans were generated. Peak-to-valley dose ratios (PVDRs) and the doses delivered to the vertices, the CTVboost, and OARs were compared among the 3 plans.

Results: The mean PVDR_{min} values for the photon, proton, and carbon-ion LRT plans were 4.78 (range, 4.34 to 5.36), 4.82 (range, 4.15 to 5.37), and 4.69 (range, 4.31 to 5.28), respectively. The mean PVDR_{mean} values for the same plans were 3.42 (range, 3.15 to 3.79), 2.93 (range, 2.19 to 3.74), and 3.58 (range, 3.09 to 4.68), respectively. There were no significant differences between the PVDR_{min} and PVDR_{mean} values across the 3 LRT plans. Most critical organs were better protected in the proton and carbon-ion LRT plans than in the photon LRT plans. The photon LRT plans showed the highest maximum degree (D_{max}) of vertices. Furthermore, these plans did not introduce more doses to the OARs compared to the 1-fraction clinical boost plan.

Conclusions: Despite minimal differences in PVDR, proton and carbon-ion LRT plans can better protect OARs than photon LRT plans.

Keywords: Lattice radiotherapy (LRT); proton; carbon-ion; pencil beam scanning (PBS); sinonasal malignancy

Submitted Dec 08, 2021. Accepted for publication Apr 02, 2022.

doi: 10.21037/atm-21-6631

View this article at: <https://dx.doi.org/10.21037/atm-21-6631>

Introduction

Sinonasal malignancies are extremely rare, accounting for 3% of all head and neck cancers and 1% of all malignancies (1-4). These lesions are a treatment challenge as they are commonly diagnosed in the advanced stage due to the late occurrence of symptoms and their close proximity to important organs at risks (OARs) (5,6). Achieving clear surgical resection of advanced tumors is difficult, and adjuvant radiotherapy (RT) is often required. Due to the complex anatomy of the region, marginal misses or underdosing of RT to the clinical targets in order to protect the OARs may cause local failure and recurrence (7-10). Therefore, delivering high radiation doses to tumors without inducing toxicity in OARs is key to the treatment of sinonasal malignancies.

Lattice radiotherapy (LRT) is a technique that delivers highly inhomogeneous doses to tumors, increasing apoptosis by bystander effects (11-13). Furthermore, LRT can modify the immunosuppressive tumor environment, potentially enhancing the benefit of antigen-specific immunotherapy (14,15). As such, LRT is a good candidate for treating sinonasal malignancies.

By using collimated photon beams, LRT can generate dose distributions concentrated in lattice vertices with a rapid dose fall-off between the vertices (11). The use of intensity modulated radiation therapy (IMRT)/volumetric modulated arc therapy (VMAT) combined with image guiding techniques to deliver LRT can optimize normal tissue sparing and concentrated peak-to-valley dose distribution within the tumor volume, to achieve partial radiation ablation and induce the immune responses. Clinical trials using photon LRT with a VMAT delivery method for ovarian carcinosarcoma and non-small cell lung cancer have been conducted since 2015. These trials have reported that LRT results in a significant reduction in tumor size, thus helping to ensure a longer overall survival without severe OAR complications (16-19).

The proton and carbon-ion pencil beam scanning (PBS) technique can deposit a Bragg peak to each vertex through inverse planning, thus delivering a high dose to the vertex while sharply decreasing the doses between Bragg peaks. Compared to protons, carbon-ions scatter less, resulting in pencil beams with smaller full width at half maximum (FWHM) diameters when using the same spot size at the same depth. Reduced scattering may produce a higher peak-to-valley dose ratio (PVDR). Meanwhile, a carbon-ion LRT plan with a smaller FWHM may be more susceptible

to minimal respiration-induced blurring of the edge of the vertex, which may deliver a high dose outside the tumor and reduce the PVDR in the actual treatment. Therefore, image guidance in LRT for the purpose of robustness of patient setup and immobilization is essential for treatment accuracy, especially in carbon-ion LRT. Besides, image guidance before treatment can facilitate observation of the change of targets and to monitor a tumor response through the course of therapy.

Gao *et al.* (20) performed spatially fractionated (GRID) therapy for deep and shallow targets using PBS proton beams with lateral spaces of 1.0 cm and 2.0 cm in water phantoms. Based on these settings, they compared the dosimetric parameters between the PBS dose distributions and the typical photon GRID technique. They found that the proton GRID therapy provided a higher PVDR than the photon GRID technique for a deep-seated phantom target. Snider *et al.* (21) delineated 3-dimensional (3D) spherical vertices with a diameter and center-to-center (c-t-c) of 3 mm and 3 cm, respectively. Based on the targets, they delivered mono-energetic proton PBS beams to 5 tumors at different sites. The results showed that the peak dose could be achieved at 15 Gy[relative biologic effectiveness (RBE)] with a confluent valley dose across the targeted tumor of approximately 1–2 Gy(RBE). In addition, the skin could be safely protected.

This study aimed to investigate the feasibility of proton or carbon-ion LRT plans for the treatment of sinonasal malignancies. Towards this goal, the spherical vertices of 10 patients with sinonasal malignant tumors were delineated. The PVDR and doses delivered to the periphery targets and OARs were compared among the photon, proton, and carbon-ion LRTs to determine whether proton and carbon-ion beams could promote the efficacy of LRT. The LRT plans were also compared to clinical carbon-ion boost plans to determine whether LRT plans increased normal tissue complications. In addition, the modalities of proton and carbon-ion LRT delivery with image guidance were discussed in terms of treatment accuracy. We present the following article in accordance with the STROBE reporting checklist (available at <https://atm.amegroups.com/article/view/10.21037/atm-21-6631/rc>).

Methods

Study design and patient selection

For the convenience of delineation, this retrospective study

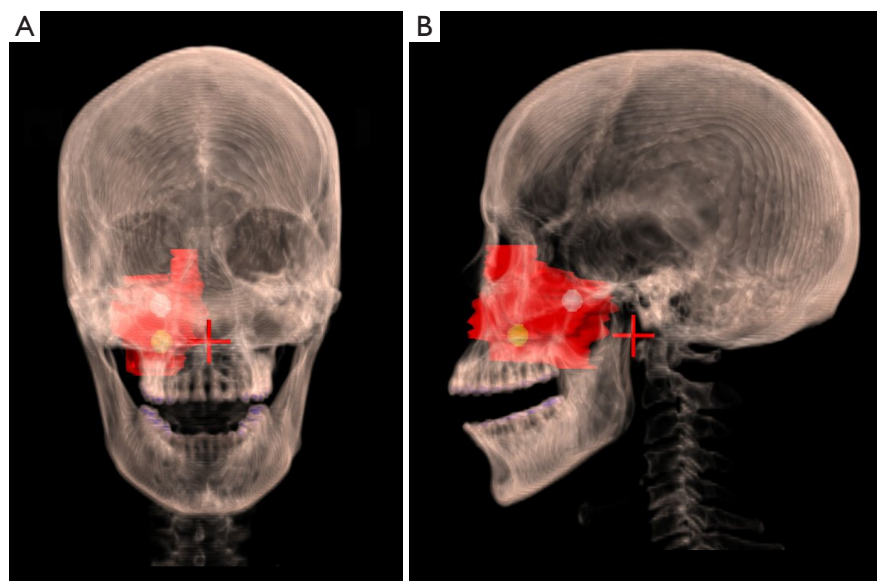


Figure 1 An example of vertex geometry within the GTV. The GTV is 72.64 cc, 2 vertices were deployed with a center-to-center distance of 3.04 cm. (A) Patterns in coronal view; (B) patterns in sagittal view. Cross mark represents the center point of the CT image. GTV, gross tumor volume.

evaluated 10 patients with bulky adenoid cystic carcinomas (ACC) who underwent biopsy and were treated with proton and carbon-ion RT at Shanghai Proton and Heavy Ion Center (SPHIC) between 2015 and 2019. Only those with the largest tumor sizes were included. The tumor diameters ranged from 6.34 to 9.58 cm (mean: 8.02 cm) in the transverse view, corresponding to a gross tumor volume (GTV) of 72.64 to 183.59 cc (mean: 120.76 cc). None of the patients underwent surgery.

Treatment planning

Description of the lattice vertices

In the treatment planning phase, the GTV and OARs were contoured in computed tomography (CT) diagnostic images. Based on the clinical contouring of OARs and targets, we additionally contoured the lattice vertices, which had a diameter of 1 cm, as suggested by Gholami *et al.* (22), noting the vertices should be kept distant from the surrounding normal tissues to avoid an ultra-high dose outside the GTV. All the vertices were within solid parts of GTVs and ensured to not overlap in the beam eye views to avoid high entrance doses, with 2–3 vertices contoured per patient. The mean c-t-c (i.e., the average distance between each vertex in the 3 dimensions) was 3.51 cm (range, 2.94 to 4.73 cm). Further, they were at least 1.6 cm apart and 1 cm away from any OAR. *Figure 1* shows an example of vertices

and the GTV of 1 patient.

Planning

For LRT, we prescribed 15 Gy(RBE) to the vertices and 3–3.5 Gy(RBE) to the periphery as the clinical target volume boost (CTVboost, with 0.5 cm expansion of GTV) in 1 fraction. Proton and carbon-ion LRT plans were generated using a 2–3 beam intensity-modulated proton (IMPT) and intensity-modulated carbon-ion (IMCT) RT with a RayStation treatment planning system (TPS) v.10A (RaySearch Laboratories, Stockholm, Sweden). The beam angles were the same for proton and carbon-ion LRT plans. The most-used beam angles in the IMPT and IMCT plans were 355°, 185°, and 275° to achieve a short incident distance and avoid the effect of the nasal and ear cavities on dose delivery. Each field covered all vertices without a range shifter. Photon LRT plans were generated using 2 full-field VMAT plan in an Eclipse TPS v. 11 (Varian Medical Systems, Palo Alto, CA, USA) with the same RT structures. The RBE of proton beams was constantly 1.1. The RBE of carbon-ions was calculated using the local effect model I, as described by Krämer and Scholz (23).

In general, patients receive 15–17.5 Gy(RBE) in 5 fractions of carbon-ion RT in CTVboost plans. In this study, the first fraction of the boost plans was replaced by a single LRT fraction, also called the LRT plan. Therefore, we assumed that the patient received a single LRT fraction

Table 1 Characteristics of the patients and vertices

Patient number	GTV (cc)	Diameter of GTV (cm)	Target depth (cm)	Number of fields in P/C LRT	Number of vertices	c-t-c distance (cm)	Vertex vol. (cc)
1	72.64	7.29	3.87	3	2	3.04	1.01
2	113.65	6.34	3.95	2	2	3.69	1.02
3	134.3	8.69	4.19	2	3	3.42	1.53
4	178.09	8.76	5.05	3	3	4.73	1.52
5	132.74	8.21	3.95	3	3	3.39	1.54
6	93.61	7.15	3.13	3	3	3.01	1.53
7	120.82	7.98	5.07	2	3	3.47	1.52
8	183.59	9.58	3.91	3	3	4.09	1.52
9	90.64	8.33	2.53	3	2	3.36	1.02
10	93.95	7.58	3.95	3	3	2.94	1.53

GTV, gross tumour volume; diameter of GTV, maximum diameter of GTV in cross section; P/C LRT, proton or carbon-ion LRT; LRT, lattice radiotherapy; c-t-c distance, center-to-center distance.

and 4 fractions of the boost plans (1 LRT + 4-fraction boost). The OAR constraints for a single LRT fraction referred to the doses of OARs in 1 fraction of boost plans and were the same for all 3 modalities. The maximum degree (D_{\max}) was <1.5 Gy(RBE) for the brainstem, <0.6 – 3 Gy(RBE) for the chiasm, and (depending on the distance to CTVboost) <1 – 3 Gy(RBE) for the optic nerves, <1.8 – 2.6 Gy(RBE) for the eyes, <1 Gy(RBE) for the lens, <5 Gy(RBE) for the skin, and <2.5 Gy(RBE) for the brain. All these dose constraints were for the single fraction. The IMPT and IMCT plans were optimized using multi-field optimization. The patient characteristics and vertex details are listed in *Table 1*.

Dose comparisons

The photon, proton, and carbon-ion LRT plans were compared with respect to the PVDRs and the doses delivered to the OARs, the vertices, and the CTVboost. The LRT plans were also compared to the 1-fraction boost plans because the doses to the OARs needed to be similar between the LRT plans, especially with respect to the IMPT and IMCT and 1-fraction boost plans, to ensure similar toxicity probabilities.

The peak volume was defined as the sum of the volumes of all vertices. The valley region was derived from the GTV minus the vertices with a non-uniform margin of 1 cm in the proton and carbon-ion beam directions and 0.7 cm

in the other directions, and was the same in the photon, proton, and carbon-ion plans for each case. We used 0.7 cm because the median distance from the 50% isodose delivered to the vertex boundary in the photon plans was 0.66 cm (range, 0.38 to 0.87 cm). Meanwhile, 1.0 cm was used due to the limitation of the beam angles. Specifically, the proton and carbon-ion LRTs had high entrance doses, with the carbon-ion LRT plan needing 1.18 cm (range, 0.22 to 4.61 cm) to lower the isodoses from 100% to 50%.

The PVDR was calculated using 2 methods. The first method was calculated based on the following Eq. [1]:

$$PVDR_{\min} = \frac{D_{\max}^{\text{peak}}}{D_{95}^{\text{valley}}} \quad [1]$$

where D_{\max}^{peak} is the median D_{\max} of each vertex, and D_{95}^{valley} is the dose covering 95% of the valley region, which is the approximate minimum dose of the valley region. The second method is shown in Eq. [2]:

$$PVDR_{\text{mean}} = \frac{D_{\text{mean}}^{\text{peak}}}{D_{\text{mean}}^{\text{valley}}} \quad [2]$$

where $D_{\text{mean}}^{\text{valley}}$ and $D_{\text{mean}}^{\text{peak}}$ are the mean doses of the valley and peak region, respectively. It has been shown that high PVDRs and low valley doses can better spare normal tissues (24).

Several variables, including the D_{\max} for the brain stem, chiasm, optic nerves, lens, spinal cord, skin, brain, and

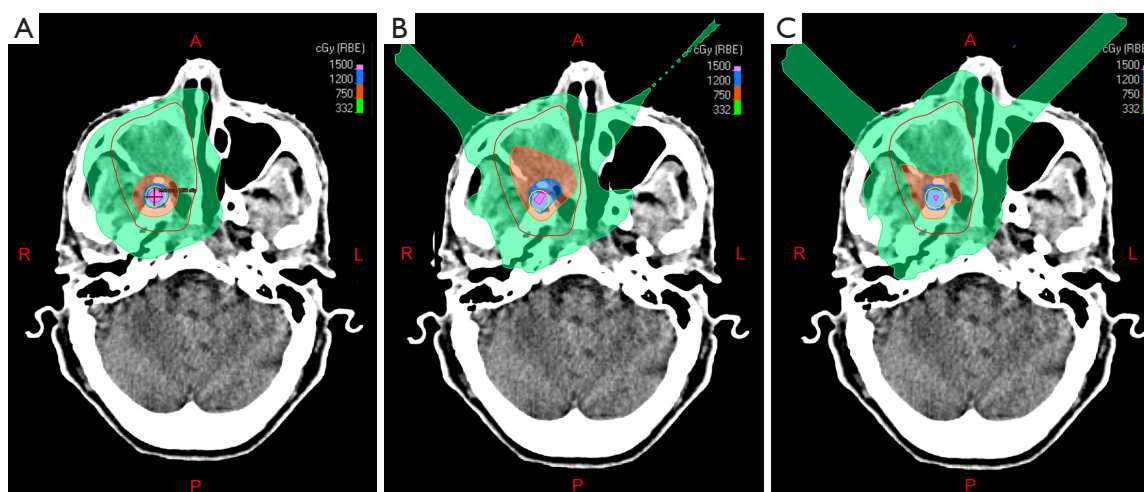


Figure 2 Comparison of dose distributions among photon, proton, and carbon-ion LRT plans. This patient has a GTV of 72.64 cc, 2 vertices, and 3.04 cm center-to-center distance. The prescribed dose of the LRT plan was 15 Gy(RBE) to the vertices and 3.5 Gy(RBE) in 1 fraction to the periphery as CTVboost. The red outline represents GTV and the yellow outline represents vertices. (A) Dose distribution of photon LRT plan; (B) dose distribution of proton LRT plan; (C) dose distribution of carbon-ion LRT plan. A, anterior; P, posterior; L, left; R, right; RBE, relative biologic effectiveness; LRT, lattice radiotherapy; GTV, gross tumor volume; CTVboost; clinical target volume boost.

vertices, the D_{mean} for the eyes, parotids, oral cavity, and brain, and the volume that received a minimum of 95% of the prescribed dose (V_{95}) of the CTVboost, were assessed for all 3 types of LRT plans. These parameters were also compared between 1 fraction of boost plans and LRT plans to determine whether the LRT plans were likely to induce potential OAR complications.

Statistical analysis

The PVDRs and doses to the vertices and targets of the 3 types of LRT plans were analyzed using the software SPSS 20.0 (IBM Corp., Chicago, IL, USA). Data between the 2 types of plans were compared using the Wilcoxon rank-sum test. A P value of <0.05 was considered statistically significant.

Delivery with image guidance

After plan generation, the LRT plan was verified in a water phantom with a 24-pinpoint chamber array. At least 22 out of 24 chambers were required to pass the gamma index criterion of 3%/3 mm. Before treatment, an off-line review CT was acquired on the same day of the scheduled LRT treatment. Based on this CT, an off-line dose evaluation was performed. If the OAR doses were acceptable, a patient

was eligible for the treatment; if not, an off-line adaptive plan was implemented to secure the OAR doses. A newly generated plan was verified by a Monte Carlo (MC) dose verification tool. During the treatment, 2-dimensional X-ray images were used to assure the patient setup was based on bone anatomy registration. If an off-line adaption was performed, the treatment plan was verified afterwards by the aforementioned water phantom with a pinpoint chamber array.

Ethical statement

The study was conducted in accordance with the Declaration of Helsinki (as revised in 2013). The study was approved by institutional review board (IRB) of Shanghai Proton and Heavy Ion Center (No. 200220EXP-02) and individual consent for this retrospective analysis was waived.

Results

Comparison of dose distributions

Figure 2 shows an example of dose distribution in the photon, proton, and carbon-ion LRT plans for 1 case. The doses from the 3 LRT plans were distributed centrally in the vertices and lowered quickly outside the vertices.

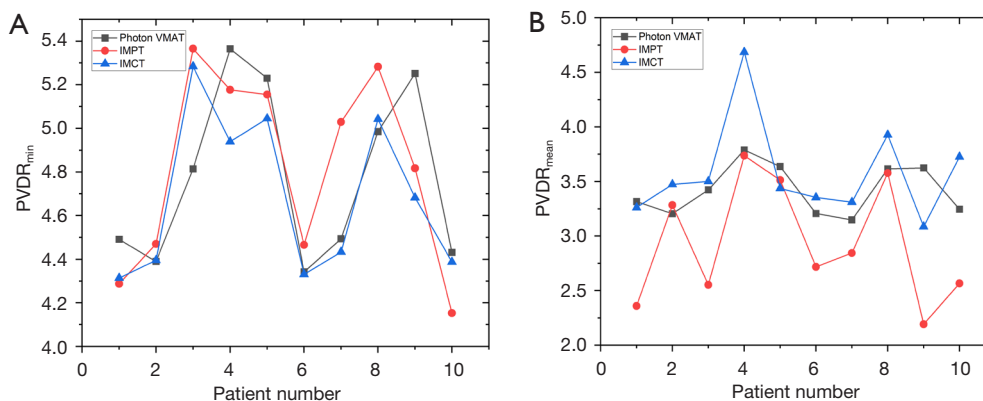


Figure 3 Comparison of PVDR_{min} and PVDR_{mean} among IMCT, IMPT, and photon VMAT plans. (A) Comparisons of PVDR_{min}. (B) Comparisons of PVDR_{mean}. PVDR, peak-to-valley dose ratio; VMAT, volumetric modulated arc therapy; IMPT, intensity-modulated proton; IMCT, intensity-modulated carbon-ion therapy.

PVDRs

The PVDR_{min} and PVDR_{mean} values were compared between the proton and carbon-ion LRT plans and the photon LRT plans (Figure 3). The mean PVDR_{min} values of the photon, proton, and carbon-ion LRT plans were 4.78 (range, 4.34 to 5.36), 4.82 (range, 4.15 to 5.37), and 4.69 (range, 4.31 to 5.28), respectively. Meanwhile, the mean PVDR_{mean} values for the same plans were 3.42 (range, 3.15 to 3.79), 2.93 (range, 2.19 to 3.74), and 3.58 (range, 3.09 to 4.68), respectively. There were no significant differences between the PVDR values of the photon, proton, and carbon-ion LRT plans: for the photon versus proton LRT plans, $P=0.912$ for PVDR_{min} and $P=0.063$ for PVDR_{mean}; for the photon versus carbon-ion LRT plans, $P=0.436$ for PVDR_{min} and $P=0.481$ for PVDR_{mean}; and for the proton versus carbon-ion plans, $P=0.436$ for PVDR_{min} and $P=0.052$ for PVDR_{mean}.

Comparison between LRT plans and between 1-fraction boost and LRT plans

The dose statistics of the variables from the photon, proton, and carbon-ion LRT plans are summarized in Table 2. There was no difference between the proton and carbon-ion LRT plans, and they showed advantages over the photon LRT plans in protecting the brain stem, chiasm, optic nerve, parotids, spinal cord, and brain. With respect to the dose delivered to targets, the photon LRT plans showed a higher V_{95} of the CTVboost than the proton LRT plans. Furthermore, there were differences between the plans in

the dose distributions of the vertices: for the proton versus carbon-ion plans, $P=0.029$ for $V_{15 \text{ Gy(RBE)}}$ of the vertices and for the photon versus proton plans, $P=0.023$ for $V_{14 \text{ Gy(RBE)}}$ of the vertices. The photon LRT plans showed the highest D_{max} of the vertices among the 3 LRT plans, with $P=0.019$ for the photon versus proton plans and $P=0.015$ for the photon versus carbon-ion plans.

Comparisons of the variables between the IMCT, IMPT, VMAT, and 1-fraction boost LRT plans are summarized in Table 3. There was no significant difference in the dose to OARs and CTVboosts between the 1-fraction boost plans and the proton or carbon-ion LRT plans, but the proton or carbon-ion LRT plans showed lower D_{max} of the brain than the 1-fraction boost plans: $P=0.009$ for the IMCT LRT plans versus 1-fraction boost plans and $P=0.041$ for the IMPT LRT plans versus 1-fraction boost plans. Meanwhile, the photon LRT plans delivered apparently higher doses to normal tissues than the 1-fraction boost plans.

Discussion

In this study, we delineated vertices for ACC patients. Photon, proton, and carbon-ion LRT plans were generated based on the vertices and peripheral target volumes. To our knowledge, this was the first study to investigate the differences of dosimetry between photon, proton, and carbon-ion LRT plans. Our results provide compelling evidence for proton and carbon-ion LRT as 1-fraction boost treatment, achieving 95% dose coverage of the CTVboost and better protection of OARs than the photon LRT plans.

Since its introduction in 2010, photon LRT has been

Table 2 Dosimetric comparisons of OARs among the three types of LRT plans

Structure	Dose-volume indices	Photon VMAT	IMPT	IMCT	P value		
					VMAT-IMPT	VMAT-IMCT	IMPT-IMCT
Brain stem	D _{max}	2.52 (1.96–3.18)	0.88 (0.03–1.68)	0.75 (0.03–1.57)	0.000	0.000	0.596
Chiasm	D _{max}	2.61 (1.76–3.14)	1.61 (0.28–3.05)	1.59 (0.25–3.03)	0.016	0.009	0.821
Optic nerve	D _{max}	2.79 (2.29–3.15)	2.00 (0.83–3.00)	1.90 (0.92–2.95)	0.013	0.013	0.473
Lens	D _{max}	1.92 (0.91–3.14)	1.27 (0.02–2.76)	1.23 (0.02–2.82)	0.112	0.082	0.677
Left parotid	D _{mean}	1.32 (0.79–2.85)	0.69 (0.01–2.02)	0.69 (0.07–1.84)	0.049	0.041	0.791
Right parotid	D _{mean}	1.24 (0.59–1.81)	0.41 (0.00–1.03)	0.48 (0.04–1.04)	0.001	0.002	0.622
Spinal cord	D _{max}	1.55 (0.98–2.54)	0.15 (0.00–0.55)	0.15 (0.01–0.46)	0.000	0.000	0.705
Skin	D _{max}	4.31 (1.17–6.24)	4.35 (2.86–5.86)	4.74 (2.86–5.97)	0.734	0.199	0.307
Brain	D _{max}	4.21 (3.62–5.85)	2.85 (1.68–3.66)	2.69 (1.71–3.47)	0.006	0.002	0.406
	D _{mean}	0.77 (0.54–1.08)	0.31 (0.11–0.49)	0.28 (0.11–0.49)	0.002	0.002	0.608
CTVboost	V _{95%} (%)	98.01 (92.53–99.96)	95.69 (90.49–99.13)	96.82 (90.37–99.85)	0.023	0.257	0.131
Vertices	D _{max}	16.28 (15.11–17.45)	16.10 (15.34–17.73)	15.58 (14.83–16.54)	0.019	0.015	0.247
	V _{15 Gy(RBE)}	20.97 (7.85–42.13)	38.25 (12.54–67.00)	25.46 (10.50–54.00)	0.110	0.247	0.029
	V _{14 Gy(RBE)}	55.02 (34.88–80.90)	72.79 (29.00–95.00)	64.35 (34.00–86.00)	0.023	0.247	0.315
	V _{13 Gy(RBE)}	91.61 (74.15–99.94)	88.19 (48.50–99.21)	84.18 (56.58–97.33)	0.739	0.190	0.436

OAR, organ of risk; LRT, Lattice radiotherapy; VMAT, volumetric modulated arc therapy; IMPT, intensity-modulated proton radiotherapy; IMCT, intensity-modulated carbon-ion radiotherapy; VMAT-IMPT, comparisons between photon VMAT plans and IMPT plans; VMAT-IMCT, comparisons between photon VMAT plans and IMCT plans; IMPT-IMCT, comparisons between IMPT plans and IMCT plans; CTVboost, clinical target volumes boost; D_{mean}, mean dose; D_{max}, maximum dose (point and/or in a significant volume); V_{95%}, the percent of volume that received a minimum of 95% of the prescribed dose to CTVboost [2.85 or 3.33 Gy(RBE)]; V₁₅, the percent of volume that received a minimum of 15 Gy(RBE); V₁₄, the percent of volume that received a minimum of 14 Gy(RBE); V₁₃, the percent of volume that received a minimum of 13 Gy(RBE).

performed in over 150 patients with advanced bulky tumors treated mainly at 2 centers: the Innovative Cancer Institute (Miami, FL, USA) and the Fujian Union Hospital (Fuzhou, China) (11,25). While it has been used in combination with conventional RT or chemotherapy, LRT has been established as the main contributor to further reductions in tumor size and longer patient survival without the addition of significant morbidity or toxicity (16,18,19). Although recent clinical trials have shown remarkable success, they have still used a photon beam, which delivers a high integral dose (usually 15–20 Gy). Several studies have reported that proton or carbon PBS provides better dosimetry over photons (26,27). The combination of LRT with proton or carbon-ion RT is a new research direction that is playing a role in the protection of OARs with a more integral dose distribution. Thus, we performed a comparative study to characterize the potential benefits of proton and carbon-ion LRTs.

Creating localized high-dose islands and low-dose valleys within the tumor volume is a basic principle of LRT; however, the dose to surrounding organs limits the use of LRT in current photon beam technologies. To overcome this limitation, proton and carbon-ion technologies were introduced, but only proton-based GRID therapy has been studied (20,21), which has revealed that the entrance dose in the proton GRID plan is high, and the beam angles are limited. Strongly grounded in GRID therapy, LRT can produce a highly concentrated dose distribution but with added flexibility in 3 dimensions. This may reduce the entrance dose and maintain the conventional dose to the surrounding OARs.

The characteristics of the vertices in our study were set in reference to those defined in a previous study of over 150 photon LRT cases (25). In that study, the average diameter of the vertex for 150 patients was 1.02 cm (0.87–1.50 cm) and

Table 3 Comparison of calculated doses between 1-fraction boost and LRT plans

Structure	Dose-volume indices	1-fraction boost plans	P value		
			IMCT-boost	IMPT-boost	VMAT-boost
Brain stem	D _{max}	1.19 (0.02–2.09)	0.096	0.289	0.000
Chiasm	D _{max}	1.74 (0.43–2.78)	0.273	0.326	0.000
Optic nerves	D _{max}	1.93 (0.87–3.00)	0.450	1.000	0.002
Lens	D _{max}	0.83 (0.05–1.54)	0.705	0.325	0.001
Left parotid	D _{mean}	0.51 (0.03–1.85)	0.364	0.705	0.013
Right parotid	D _{mean}	0.54 (0.01–1.58)	0.705	0.705	0.019
Spinal cord	D _{max}	0.30 (0.01–0.70)	0.241	0.120	0.000
Brain	D _{max}	3.52 (3.20–3.93)	0.009	0.041	0.048
	D _{mean}	0.19 (0.03–0.33)	0.337	0.142	0.002
Left eye	D _{mean}	0.79 (0.08–1.66)	0.199	0.241	0.003
Right eye	D _{mean}	0.60 (0.00–1.86)	0.307	0.496	0.006
CTVboost	V _{95%}	97.40 (92.33–99.43)	0.529	0.075	0.579

The prescription of 1-fraction boost plans: 3–3.5 Gy(RBE) to CTVboost; the prescription of LRT plans, 15 Gy(RBE) to vertices and 3–3.5 Gy(RBE) to CTVboost. LRT, lattice radiotherapy; IMCT, intensity-modulated carbon-ion radiotherapy; IMPT, intensity-modulated proton radiotherapy; VMAT, volumetric modulated arc therapy; CTVboost, clinical target volumes boost; D_{max}, maximum dose; D_{mean}, mean dose; V_{95%}, volume that received a minimum of 95% of the prescribed dose [2.85 or 3.33 Gy(RBE)].

the c-t-c was approximately 2–5 cm. With smaller vertex sizes and narrower separations, it is possible to achieve a higher PVDR with less scatter of proton and carbon-ions than of photons. Further research is needed to validate the optimal characteristics of the vertices in proton and carbon-ion LRT plans.

The PVDR calculated in this study was based on the valley regions, which were defined as the volume with less than 50% of the prescription dose within the GTV. Amendola *et al.* (19) delivered 18.00 Gy to vertices and 3.00 Gy to peripheral GTV using photon beams. The average dose falloff in their study from 18.00 Gy (100%) to 6.66 Gy (37%) was 3.6 cm, which was more than the c-t-c distance in our study (i.e., 3.51 cm). Thus, our valley doses had to be higher than their criteria. Finally, we assumed that the valley dose was 7.5 Gy (50%) of the LRT prescription.

A high PVDR is the key objective of successful LRT for large tumors. The small difference in the PVDR among scattered photons, protons, and carbon-ions was a result of the large PBS spot size caused by the low energy when treating shallow tumors and the fewer fields in the proton and carbon-ion plans than the photon plans. This leads to comparable PVDRs between the photon, proton, and carbon-ion LRT plans. Concurrently, less lateral scattering

of particle beams, especially carbon-ion beams, enables lower doses to the OARs in the proton and carbon-ion plans while the fewer fields result in high doses delivered to the skin in the proton and carbon-ion plans.

It is possible to use LRT to induce immune responses through its high-dose component, including abscopal and bystander effects. The presence of a bystander in GRID has been experimentally documented by a significant decrease in clonogenic survival and an increase in the expression of DNA-damaged genes in bystander cells (14,28). Larger tumors may release more antigens in response to irradiation, which potentially intensifies the abscopal effects (29). Furthermore, the combination of RT and immunotherapy can enhance T cell infiltration and inhibition of myeloid-derived suppressor cells and regulatory T cells (30). As such, many factors, including the characteristics of vertices and radiation sequence, need to be further explored to augment the immunogenic responses.

Carbon-ion beams with high linear energy transfer values have been shown to possess higher RBE and induce more complex DNA damage. Importantly, they cause a significant reduction in radioresistance (31–35). Meanwhile, carbon-ion beams may lead to radiation-induced bystander effects and abscopal effects in high-dose irradiation of

partial tumors. These effects may be induced in a different manner compared to that of photons, as reported in an animal model study (36). However, the advantage of carbon-ion beams is yet to be investigated. We believe that it is imperative to conduct this dosimetric comparison and thus conducted it as part of this study.

Sinonasal malignancies are not tractable by conventional radiation due to the sensitive surrounding OARs. In contrast to conventional photon beam RT, LRT with carbon ions can better deliver high-dose radiation to the target tumor. Further, it can induce bystander effects and abscopal effects to increase apoptosis in the peripheral tumor cells while having no adverse effects on adjacent organs, as indicated in our study. Therefore, LRT with carbon-ions is an advantageous option as a 1-fraction boost plan to treat sinonasal malignant tumors.

The first step in proton and carbon-ion LRT is the delineation of vertices. In our study, the vertices were contoured based on the geometry of GTVs. However, placement of vertices within hypoxic volume may increase the immunological potential. High-spatial resolution positron emission tomography (PET) imaging with a hypoxia-specific tracer has been shown to be a useful tool to accurately characterize tumor oxygenation (37), and may be a good candidate in vertices delineation in the future. Quality assurance should be conducted before treatment to verify the absolute dose; in this study, the pinpoint chamber array was proposed to verify the LRT plan in a water phantom, and an MC tool was used for fast-plan verification. Image guidance before and during LRT treatment for patient setup and repositioning is necessary to ensure tumor coverage and high dose concentration.

With regards to these image guidance techniques, a new workflow of proton and carbon-ion LRT is proposed for further study, as below. The PET imaging is implemented for vertices delineation. After vertices delineation, plans are generated and the verification of doses occurs with the chambers, including a review CT, which is acquired on the same day as the LRT treatment day and used to account for anatomic changes and to perform adaptive therapy when needed. The newly generated plans are also approved by verification. During treatment, cone beam (CB)CT or in-room CT is used for patient setup and repositioning with 3D information, and optical surface imaging is a good candidate for patients whose tumor volumes are far away from major bony structures.

This study had some limitations. The evaluation of the LRT plans should take more factors into consideration, especially when combined with the proton and carbon-ion beams. Range uncertainty is a key problem in particle RT. Due to the limited number of beams and the complexity of patient anatomy, this problem may have been more severe in this study. Therefore, the geometrical design of the vertex and beam angle selection should have been approached more cautiously. With the valley dose in the proton and carbon-ion plans expected to be lower than 50% of the prescribed dose, which is different from that in the photon LRT clinical trial of Amendola *et al.* (19), the clinical or biological outcomes may not be similar. Meanwhile, the different isodose volumes of the high-dose region, 13, 14, and 15 Gy(RBE), and the larger drop off region due to the high-entrance dose in proton and carbon-ion plans could alter clinical responsiveness. Accordingly, clinical trials should be undertaken to verify the clinical outcomes of proton and carbon-ion LRT. Meanwhile, the exact mechanism of how LRT exerts a killing effect on tumors remains to be studied. Molecular imaging may help us understand treatment regimens, tumor control, and toxicity outcomes of LRT. In this study, a logical effect model (LEM) was used to calculate the RBE-weighted carbon-ion LRT. Whether this model can accurately predict the RBE of carbon ions at such a high dose level remains to be seen. The RBE for proton plans was constantly 1.1, while the RBE was slightly increased in peak regions, which can cause the peak equivalent dose for proton plans to be higher, reducing the effectiveness of PVDR. Thus, the prescribed doses may not have been clinically equivalent for the 3 modalities. The future of proton and carbon-ion LRT requires a workflow which includes the principle of delineation, the standard for treatment planning, the validation of doses, accurate imaging for treatment planning, image guidance for treatment delivery, and the observation and exploration of in-vivo effects. The results stated in this study were appropriately made in the case of an evaluation of nominal plans of photons, protons, and carbon ions. In a clinical situation, the appropriateness of a particle beam plan must also include comments on the effects of range and set-up errors to the dose distribution, compared to the nominal plan. Only when evaluation occurs with range and set-up errors maintained according to acceptable criteria, can the comparisons between photons, protons, and carbon-ion plans be considered safe

for delivery in a clinical situation.

Conclusions

Dosimetric comparisons of photon, proton, and carbon-ion LRT plans showed no significant difference in PVDR. However, proton and carbon-ion LRT plans can protect OARs better than photon LRT plans. This was also confirmed by comparing doses delivered to OARs and the CTVboost between 1-fraction boost plans and LRT plans. Therefore, a prospective clinical study is warranted to evaluate the efficacy of proton or carbon-ion LRT plans for the treatment of sinonasal malignancies, particularly in terms of tumor control and toxicity of normal tissues.

Acknowledgments

Funding: This work was supported by the Program of Shanghai Academic/Technology Research Leader (18XD1423000).

Footnote

Reporting Checklist: The authors have completed the STROBE reporting checklist. Available at <https://atm.amegroups.com/article/view/10.21037/atm-21-6631/rc>

Data Sharing Statement: Available at <https://atm.amegroups.com/article/view/10.21037/atm-21-6631/dss>

Conflicts of Interest: All authors have completed the ICMJE uniform disclosure form (available at <https://atm.amegroups.com/article/view/10.21037/atm-21-6631/coif>). All authors report funding from the Program of Shanghai Academic/Technology Research Leader (18XD1423000).

Ethical Statement: The authors are accountable for all aspects of the work in ensuring that questions related to the accuracy or integrity of any part of the work are appropriately investigated and resolved. The study was conducted in accordance with the Declaration of Helsinki (as revised in 2013). The study was approved by institutional review board (IRB) of Shanghai Proton and Heavy Ion Center (No. 200220EXP-02) and individual consent for this retrospective analysis was waived.

Open Access Statement: This is an Open Access article

distributed in accordance with the Creative Commons Attribution-NonCommercial-NoDerivs 4.0 International License (CC BY-NC-ND 4.0), which permits the non-commercial replication and distribution of the article with the strict proviso that no changes or edits are made and the original work is properly cited (including links to both the formal publication through the relevant DOI and the license). See: <https://creativecommons.org/licenses/by-nc-nd/4.0/>.

References

1. Haerle SK, Gullane PJ, Witterick IJ, et al. Sinonasal carcinomas: epidemiology, pathology, and management. *Neurosurg Clin N Am* 2013;24:39-49.
2. Turner JH, Reh DD. Incidence and survival in patients with sinonasal cancer: a historical analysis of population-based data. *Head Neck* 2012;34:877-85.
3. Cooper JS, Porter K, Mallin K, et al. National Cancer Database report on cancer of the head and neck: 10-year update. *Head Neck* 2009;31:748-58.
4. Kawaguchi M, Kato H, Tomita H, et al. Imaging Characteristics of Malignant Sinonasal Tumors. *J Clin Med* 2017;6:116.
5. Jakobsen MH, Larsen SK, Kirkegaard J, et al. Cancer of the nasal cavity and paranasal sinuses. Prognosis and outcome of treatment. *Acta Oncol* 1997;36:27-31.
6. Sakata K, Aoki Y, Karasawa K, et al. Analysis of the results of combined therapy for maxillary carcinoma. *Cancer* 1993;71:2715-22.
7. Terhaard CH, Lubsen H, Rasch CR, et al. The role of radiotherapy in the treatment of malignant salivary gland tumors. *Int J Radiat Oncol Biol Phys* 2005;61:103-11.
8. Garden AS, Weber RS, Ang KK, et al. Postoperative radiation therapy for malignant tumors of minor salivary glands. Outcome and patterns of failure. *Cancer* 1994;73:2563-9.
9. Chen AM, Bucci MK, Weinberg V, et al. Adenoid cystic carcinoma of the head and neck treated by surgery with or without postoperative radiation therapy: prognostic features of recurrence. *Int J Radiat Oncol Biol Phys* 2006;66:152-9.
10. Geara FB, Sanguineti G, Tucker SL, et al. Carcinoma of the nasopharynx treated by radiotherapy alone: determinants of distant metastasis and survival. *Radiother Oncol* 1997;43:53-61.
11. Wu X, Ahmed MM, Wright J, et al. On modern technical approaches of three-dimensional high-dose Lattice

- radiotherapy (LRT). *Cureus* 2010;2:e9.
12. Kanagavelu S, Gupta S, Wu X, et al. In vivo effects of lattice radiation therapy on local and distant lung cancer: potential role of immunomodulation. *Radiat Res* 2014;182:149-62.
 13. Pellizzon ACA. Lattice radiation therapy - its concept and impact in the immunomodulation cancer treatment era. *Rev Assoc Med Bras (1992)* 2020;66:728-31.
 14. Asur R, Butterworth KT, Penagaricano JA, et al. High dose bystander effects in spatially fractionated radiation therapy. *Cancer Lett* 2015;356:52-7.
 15. Yakovlev VA. Role of nitric oxide in the radiation-induced bystander effect. *Redox Biol* 2015;6:396-400.
 16. Amendola BE, Perez NC, Wu X, et al. Improved outcome of treating locally advanced lung cancer with the use of Lattice Radiotherapy (LRT): A case report. *Clin Transl Radiat Oncol* 2018;9:68-71.
 17. Amendola BE, Perez N, Amendola MA, et al. Lattice radiotherapy with RapidArc for treatment of gynecological tumors: Dosimetric and early clinical evaluations. *Cureus* 2010;2:e15
 18. Blanco Suarez JM, Amendola BE, Perez N, et al. The Use of Lattice Radiation Therapy (LRT) in the Treatment of Bulky Tumors: A Case Report of a Large Metastatic Mixed Mullerian Ovarian Tumor. *Cureus* 2015;7:e389.
 19. Amendola BE, Perez NC, Wu X, et al. Safety and Efficacy of Lattice Radiotherapy in Voluminous Non-small Cell Lung Cancer. *Cureus* 2019;11:e4263.
 20. Gao M, Mohiuddin MM, Hartsell WF, et al. Spatially fractionated (GRID) radiation therapy using proton pencil beam scanning (PBS): Feasibility study and clinical implementation. *Med Phys* 2018;45:1645-53.
 21. Snider JW, Diwanji T, Langen KM. A Novel Method for the Delivery of 3-Dimensional High-Dose Spatially Fractionated Radiation Therapy with Pencil Beam Scanning Proton Therapy: Maximizing the Benefit of the Bragg Peak. *Int J Radiat Oncol Biol Phys* 2017;99:S232-33.
 22. Gholami S, Nedaie HA, Longo F, et al. Grid Block Design Based on Monte Carlo Simulated Dosimetry, the Linear Quadratic and Hug-Kellerer Radiobiological Models. *J Med Phys* 2017;42:213-21.
 23. Krämer M, Scholz M. Treatment planning for heavy-ion radiotherapy: calculation and optimization of biologically effective dose. *Phys Med Biol* 2000;45:3319-30.
 24. Zwicker RD, Meigooni A, Mohiuddin M. Therapeutic advantage of grid irradiation for large single fractions. *Int J Radiat Oncol Biol Phys* 2004;58:1309-15.
 25. Wu X, Perez NC, Zheng Y, et al. The Technical and Clinical Implementation of LATTICE Radiation Therapy (LRT). *Radiat Res* 2020;194:737-46.
 26. Elsässer T, Weyrather WK, Friedrich T, et al. Quantification of the relative biological effectiveness for ion beam radiotherapy: direct experimental comparison of proton and carbon ion beams and a novel approach for treatment planning. *Int J Radiat Oncol Biol Phys* 2010;78:1177-83.
 27. Hu J, Huang Q, Gao J, et al. Clinical outcomes of carbon-ion radiotherapy for patients with locoregionally recurrent nasopharyngeal carcinoma. *Cancer* 2020;126:5173-83.
 28. Protopapa M, Kouloulis V, Kougioumtzopoulou A, et al. Novel treatment planning approaches to enhance the therapeutic ratio: targeting the molecular mechanisms of radiation therapy. *Clin Transl Oncol* 2020;22:447-56.
 29. Wang R, Zhou T, Liu W, et al. Molecular mechanism of bystander effects and related abscopal/cohort effects in cancer therapy. *Oncotarget* 2018;9:18637-47.
 30. Persa E, Balogh A, Sáfrány G, et al. The effect of ionizing radiation on regulatory T cells in health and disease. *Cancer Lett* 2015;368:252-61.
 31. Dokic I, Mairani A, Niklas M, et al. Next generation multi-scale biophysical characterization of high precision cancer particle radiotherapy using clinical proton, helium-, carbon- and oxygen ion beams. *Oncotarget* 2016;7:56676-89.
 32. Klein C, Dokic I, Mairani A, et al. Overcoming hypoxia-induced tumor radioresistance in non-small cell lung cancer by targeting DNA-dependent protein kinase in combination with carbon ion irradiation. *Radiat Oncol* 2017;12:208.
 33. Valable S, Gérault AN, Lambert G, et al. Impact of Hypoxia on Carbon Ion Therapy in Glioblastoma Cells: Modulation by LET and Hypoxia-Dependent Genes. *Cancers (Basel)* 2020;12:2019.
 34. Furusawa Y, Fukutsu K, Aoki M, et al. Inactivation of aerobic and hypoxic cells from three different cell lines by accelerated (3)He-, (12)C- and (20)Ne-ion beams. *Radiat Res* 2000;154:485-96.
 35. Tinganelli W, Ma NY, Von Neubeck C, et al. Influence of acute hypoxia and radiation quality on cell survival. *J Radiat Res* 2013;54 Suppl 1:i23-30.
 36. Huang Q, Sun Y, Wang W, et al. Biological Guided

Carbon-Ion Microporous Radiation to Tumor Hypoxia Area Triggers Robust Abscopal Effects as Open Field Radiation. *Front Oncol* 2020;10:597702.

37. Thorwarth D, Geets X, Pausco M. Physical radiotherapy treatment planning based on functional PET/CT data. *Radiother Oncol* 2010;96:317-24.

Cite this article as: Yang D, Wang W, Hu J, Hu W, Zhang X, Wu X, Lu JJ, Kong L. Feasibility of lattice radiotherapy using proton and carbon-ion pencil beam for sinonasal malignancy. *Ann Transl Med* 2022;10(8):467. doi: 10.21037/atm-21-6631